## Supplementary information for

# Rational stabilization of helix 2 of the prion protein prevents its misfolding and oligomerization

Jogender Singh, Harish Kumar, Ambadi T. Sabareesan and Jayant B. Udgaonkar*

National Centre for Biological Sciences
Tata Institute of Fundamental Research
Bengaluru 560065, India

Corresponding author: Jayant B. Udgaonkar
National Centre for Biological Sciences
Tata Institute of Fundamental Research
Bengaluru 560065, India
Email: jayant@ncbs.res.in
Fax: 91-80-23636662

**Materials and methods:**

**Reagents.** All reagents used for experiments were of the highest purity grade available from Sigma, unless otherwise specified. Urea and GdnHCl were purchased from USB, and were of the highest purity grade.

**Site-directed mutagenesis.** The mutant variants of the full-length mouse prion protein (moPrP) were generated using the QuikChange® site-directed mutagenesis kit (Stratagene). Primers containing 3-6 nucleotide changes were obtained from Sigma. The mutations in the plasmids were confirmed by DNA sequencing.

**Protein expression and purification.** moPrP and all the mutant variants were expressed in *Escherichia coli* BL21 (DE3) codon plus (Stratagene) cells upon transformation with a pET17b plasmid containing the full-length sequence (23–231) of the moPrP gene. All the moPrP variants were purified as described previously.[1] No reducing agent was used during the whole protein purification procedure, and only one peak for the prion protein was observed during the reverse-phase chromatography step of protein purification. The protein that eluted out in this peak was in the oxidized disulphide containing form as checked by mass spectrometry. The purity of all the moPrP variant preparations was confirmed by mass spectrometry (Waters Synapt G2 mass spectrometer).

**Oxidation status of the cysteine residues of the moPrP variants.** To check the oxidation status of the cysteine residues, all the moPrP variants were first unfolded in 6 M GdnHCl, 50 mM Tris-HCl at pH 8, so that the cysteine residues became completely solvent accessible. The unfolded proteins were then treated with a 100-fold molar excess of 5,5′-dithiobis(2-nitrobenzoic acid) (DTNB) for 1 h. The protein samples were then desalted by reverse-phase chromatography using a Resource RPC column. The masses of the desalted protein samples were determined by mass spectrometry (Waters Synapt G2 mass spectrometer). The masses of all the moPrP variants remain unchanged after DTNB treatment, indicating that the cysteine residues were present not in reduced form but in a disulphide bond. The oxidation status of the protein in oligomers was also checked. To this end, wt oligomers formed at pH 4 in 150 mM NaCl were treated with a 100-fold molar excess of DTNB for 1 h in 0 M and 6 M GdnHCl at pH 8. The mass of the protein was found to remain unchanged after DTNB treatment. When the prion protein was reduced by dithiothreitol (DTT) treatment, the reduced protein was found to stick to different size-exclusion chromatography columns, and hence

reduced prion protein could not be used as a control for DTNB labeling. Hence as a control, tau K19 protein, which has a single cysteine residue, was treated with a 100-fold molar excess of DTNB in 6 M GdnHCl, 50 mM Tris-HCl at pH 8. The protein was desalted using a PD-10 column (Amersham Biosciences). The extent of labeling was checked by mass spectrometry, and the protein was found to be fully labeled as judged by the observed 198 Da increase in its mass upon labeling, and the absence of any peak in the mass spectrum corresponding to the mass of the unlabeled protein.

**Far-UV Circular Dichroism (CD) measurements.** Far-UV CD spectra were collected using a Jasco J-815 spectropolarimeter. Far-UV CD spectra were acquired using a protein concentration of 10 μM in a 1 mm cuvette, using a scan speed of 50 nm/min, a digital integration time of 2 s, and a bandwidth of 1 nm.

**Denaturant-induced equilibrium unfolding studies.** Denaturant-induced equilibrium unfolding transitions were carried out at pH 4 (in 10 mM sodium acetate buffer) and at pH 7 (in 50 mM Tris-HCl buffer) using 10 μM of protein. Urea-induced unfolding was carried out at pH 4, and GdnHCl unfolding was carried out at pH 7. The samples were incubated at room temperature (25 $^{o}$C) for 2 h before monitoring the change in the far-UV CD signal at 222 nm using the Jasco J-815 spectropolarimeter. The data were fit to a two-state (N ↔ U) equilibrium unfolding model,[2] and the thermodynamic parameters were obtained.

**Thermal equilibrium unfolding studies.** Thermal equilibrium unfolding transitions were monitored at pH 4 in 10 mM sodium acetate buffer using the change in the CD signal at 222 nm on the Jasco J-815 spectropolarimeter. 10 μM protein was used in a 1 mm cuvette, and the temperature scanning rate was 1 °C/min.

**Misfolding and oligomerization at different pH values.** The protein in 10 mM sodium acetate buffer (pH 4) was diluted two-fold with 2×oligomerization buffers (containing 300 mM NaCl), so that the protein was finally in 1×oligomerization buffer containing 150 mM NaCl at the desired pH. 50 mM glycine-HCl buffer was used for pH 3.1, 10 mM sodium acetate buffer was used for pH values 3.6, 4.0, 4.4, 4.8 and 5.0 while 20 mM MES buffer was used for pH values 5.35, 5.7 and 5.95. The samples were then incubated at 37 $^{o}$ for 24 h. The final protein concentration used for all the experiments was 100 μM.

For studying the extent of misfolding, each sample was diluted to 10 μM in the same buffer in which it had been incubated for 24 h, and the far-UV CD spectrum was acquired within 15 min after dilution.

For studying the extent of oligomerization, 100 μL of 100 μM incubated sample was taken out and injected into a Waters Protein Pak 300-SW column using an Akta (GE) chromatography system. The column was first equilibrated with 4 column volumes of 1×oligomerization buffer at pH 4 (10 mM sodium acetate buffer, 150 mM NaCl). 1×oligomerization buffer at pH 4 was used as the running buffer. In all size exclusion chromatography (SEC) experiments, the amounts of oligomer and monomer that eluted out were found to account for all the protein that had been injected into the column. The areas of the monomer and oligomer peaks were calculated by fitting the SEC profiles to multiple Gaussian peaks, using Origin Pro 8. The percent monomer left was calculated from the area under the monomer peak divided by the total area under all the peaks. The percent oligomer formed was then calculated by subtracting percent monomer from 100.

For analysis of the pH dependence of the CD signal and of the extent of oligomer formation, it was assumed that the formation of the oligomer (O) was coupled to the protonation, with dissociation constant $K_a$, of a single critical residue in the monomeric protein (M).

$M + H^+ \leftrightarrow MH^+ \leftrightarrow O$

It is assumed that only $MH^+$ is competent to form O. In that case, the pH dependence is that of the protonation of M, and is given by a transformation of the Henderson-Hasselbalch equation:

$$Fraction\ MH^+ = \frac{1}{1+10^{(pH-pKa)}} \qquad \text{- (1)}$$

Fraction $MH^+$ is the fraction of protein protonated at the critical titrating residue. It is assumed that the $MH^+ \leftrightarrow O$ equilibrium completely favors O at the high protein concentration (100 μM) used. Then, Fraction $MH^+$ is equal to Fraction oligomer.

**Oligomerization at pH 4 in the absence of chemical denaturants.** The protein in 10 mM sodium acetate buffer (pH 4) was diluted two-fold with 2×oligomerization buffer (10 mM sodium acetate buffer, 300 mM NaCl, pH 4), so that the protein was finally in 1×oligomerization buffer (10 mM sodium acetate buffer, 150 mM NaCl, pH 4). The samples were then incubated at 37 $^oC$. The final protein concentration used for all the experiments was

100 μM. Oligomerization at different time-points was then monitored by SEC and the data were analyzed in the same way as for the oligomerization at different pH values. Concurrently, the samples were diluted to 10 μM in 1×oligomerization buffer and far-UV CD spectra were acquired.

**Oligomerization at pH 4 in the presence of chemical denaturants.** The protein in 10 mM sodium acetate buffer (pH 4) was diluted three-fold with 1.5×oligomerization buffer (10 mM sodium acetate buffer, 225 mM NaCl, 1.5 M GdnHCl, 4.5 M urea, pH 4), so that the protein was finally in 1×oligomerization buffer (10 mM sodium acetate buffer, 150 mM NaCl, 1 M GdnHCl, 3 M urea, pH 4). The samples were then incubated at 37 $^{o}$C. The final protein concentration used for all the experiments was 100 μM. Oligomerization at different time-points was then monitored by SEC. The column was first equilibrated with 4 column volumes of 1×oligomerization buffer (10 mM sodium acetate buffer, 150 mM NaCl, 1 M GdnHCl, 3 M urea, pH 4). The data were analyzed in the same way as for the oligomerization at different pH values.

**Oligomerization at pH 2.** Oligomerization at pH 2 was essentially carried out as shown previously.[3] Briefly, the protein in 10 mM sodium acetate buffer (pH 4) was diluted two-fold with 2×aggregation buffer (100 mM glycine-HCl buffer, 300 mM NaCl, pH 2), so that the protein was finally in 1× aggregation buffer (50 mM glycine-HCl buffer, 150 mM NaCl, pH 2). The samples were then incubated at 25 $^{o}$C. The final protein concentration used for all the experiments was 100 μM. Oligomerization at different time-points was then monitored by SEC. The column was first equilibrated with 4 column volumes of 1×aggregation buffer (50 mM glycine-HCl buffer, 150 mM NaCl, pH 2). The data were analyzed in the same way as for the oligomerization at pH 4. For far-UV CD, the samples were diluted to 10 μM in 1×oligomerization buffer, and spectra were acquired.

**Fibril formation at pH 7.** Fibrilization at pH 7 was carried out in 96-well plates in a Fluoroskan Ascent plate reader. To start fibrilization, the protein in 10 mM sodium acetate buffer (pH 4) was diluted two-fold with 2×aggregation buffer (100 mM Tris–HCl, 4 M GdnHCl, pH 7.45) so that the protein was finally in 1×aggregation buffer (50 mM Tris–HCl, 2 M GdnHCl pH 7). The final protein concentration used for all the experiments was 50 μM. 50 μM ThT was added to the reaction samples. The protein in 1×aggregation buffer was then transferred to different wells of a 96-well plate in volumes of 200 μL and was incubated at 37 °C and shaken at 480 rpm using the Fluroskan Ascent plate reader. ThT fluorescence was

measured at 475 nm upon excitation at 445 nm. ThT readings were acquired after every 10 minutes.

**Atomic force microscopy (AFM).** Samples for AFM at pH 2 and pH 7 were prepared as described earlier.[1,4] For samples at pH 4, an aliquot of aggregating protein solution was withdrawn at 3 days, diluted to 5 μM in 1×oligomerization buffer, and then applied on to freshly cleaved mica (Grade V1; SPI Supplies). The sample was allowed to incubate for 1 min on the mica, rinsed with milli-Q water three times, and then dried under vacuum for 1 h. AFM images were obtained using a PicoPlus AFM instrument (Molecular Imaging, Inc.) operating in the non-contact mode using 75 kHz, 2.8 N/m cantilevers with a rounding tip radius of < 10 nm (NanoWorld AG).

**Preparation of unilamellar liposomes and the liposome swelling assay.** Unilamellar liposomes were made from diphytanoylphosphatidylcholine (DPhPC) in 1×oligomerization buffer (10 mM sodium acetate buffer, 150 mM NaCl, pH 4) containing 3 mM dextran (10 kDa), as described earlier.[5] Dynamic light scattering measurements on a DynaPro-99 instrument (Protein Solutions) indicated that the average diameter of the vesicles was 460 ± 65 nm. Liposomes were subsequently incubated with moPrP aggregates formed at 24 h of incubation in the presence of 150 mM NaCl at 37 $^{o}$C, pH 4, for 1 h before performing the liposome swelling assay.

The pore-forming activity of moPrP aggregates was assessed by a liposome swelling assay.[5,6] The dextran containing liposomes were diluted into buffer containing PEG 1000 Da, and the absorbance at 520 nm was recorded at 1 s intervals for 10 min using a Cary 1 UV‑Visible spectrophotometer (Varian). Buffer conditions under which no absorbance change was seen with control liposomes were deemed isosmotic. The liposome mixture was stirred constantly to prevent settling and aggregation. Influx of solute into proteoliposomes results in swelling and a consequent decrease in absorbance. The limiting change in absorbance is proportional to the fraction of proteoliposomes that are permeable to the solute.

**HDX-MS measurements.** The peptide map of moPrP variants was generated as described earlier.[6] To initiate deuterium labeling, a 100 μM of protein sample was diluted 20 times in a labeling buffer at pH 4 (10 mM sodium acetate buffer in $D_2O$, corrected for isotope effect) so that the protein was in 95 % $D_2O$, and was incubated at 25 $^{o}$C. At different times of labeling, a 50 μL of aliquot was withdrawn from the labeling reaction and was mixed with 50 μL of ice-cold 20 mM glycine-HCl buffer at pH 2.5 to quench the labeling. These samples were

then immediately injected into the HDX module (Waters) coupled with a nano Acquity UPLC, for online pepsin digestion using an immobilized pepsin cartridge (Applied Biosystems). Further processing of the sample for mass determination using a Waters Synapt G2 mass spectrometer, was carried out as described earlier.[6] The parameters used for the mass spectrometer measurements and the HDX module set-up have been described earlier.[6]

Peptide masses were calculated from the centroid of the isotopic envelope using the MassLynx software, and the shift in the mass of labeled peptide relative to the unlabeled peptide was used to determine the extent of deuterium incorporation at each time point of HDX. As the samples were in 95 % $D_2O$ during labeling and were exposed to $H_2O$ after the quenching of the labeling reaction, control experiments were carried out to correct for back-exchange and forward-exchange. To this end, moPrP variants were incubated in 10 mM sodium acetate buffer at pH 4 containing 95 % $D_2O$ and were fully deuterated by unfolding at their respective $T_m$ (see Table S1 for the $T_m$ values of the different moPrP variants) for 10 min, followed by refolding on ice. The fully deuterated moPrP samples were then processed in exactly the same way as the labeling reaction sample. The extent of deuterium incorporation in each peptide, % D, was determined using the equation $\% D = (m(t) - m(0\%))/(m(95\%) - m(0\%)) \times 100$, where $m(t)$ is the measured centroid mass of the peptide at time point $t$, $m(0\%)$ is the measured mass of an undeuterated reference sample, and $m(95\%)$ is the measured mass of a fully deuterated reference sample (in 95% $D_2O$).[7] For calculation of the free energy of stabilization (ΔG), the observed HDX rate curve ($k_{obs}$) for a peptide fragment, which was obtained by fitting either to mono-exponential or bi-exponential curve depending upon the goodness of fit, was compared to a reference (intrinsic) curve ($k_{int}$) expected for the peptide in a random coil state.[8] The HDX protection factor ($Pf= k_{int}/k_{obs}$) for a peptide was used to calculate the local stability ΔG of the segment corresponding to the peptide ($\Delta G = RT \ln Pf$).

**Supplementary text:**

**Thermodynamic stability measurements of the moPrP variants.** The thermodynamic stabilities of the moPrP variants were determined both at pH 4 (Figure 1a) and pH 7 (Figure S2a). The stabilities at pH 4 were measured in urea in the absence of salt. The prion protein under these conditions is known to be present in monomeric form.[9,10] On the other hand, addition of salt in the presence of urea or use of GdnHCl as a denaturant at pH 4 leads to the formation of oligomeric forms.[9,11] At pH 7, the prion protein is known to be present in monomeric form both in urea and in GdnHCl.[11] An increased stability of the moPrP variants made it impossible to obtain unfolded protein baselines for the equilibrium denaturation curves at pH 7 in the presence of urea. Hence, GdnHCl, which is a stronger denaturant, was used to determine the thermodynamic stabilities at pH 7.

**Oxidation status of cysteine residues of the moPrP variants.** Reduction of the disulphide bond of PrP leads to destabilization of the protein.[12,13] To check whether the differences in the stabilities of the moPrP variants were due to changes in the oxidation status of the cysteine residues in the moPrP variants, DTNB treatment of the moPrP variants was carried out. DTNB will lead to the labeling of an exposed thiol group which would lead to an increase in the mass by 198 Da, but will be unable to label cysteine residues which are involved in disulphide bond formation. All the moPrP variants were unfolded in 6 M GdnHCl, 50 mM Tris-HCl at pH 8, to make the cysteine residues accessible to DTNB. The unfolded proteins were then treated with 100-fold molar excess of DTNB for an hour. The masses of all the moPrP variants remain unchanged upon DTNB treatment (Figure S3a). Similarly, when the oligomers formed by wt moPrP were treated with DTNB either in the absence or presence of 6 M GdnHCl, the mass of the protein was found to remain unchanged (Figure S3b). This result shows that the cysteine residues in the protein present in oligomers are also oxidized to form a disulphide bond. On the other hand, Tau K19 protein, which has a single cysteine, showed complete labeling (Figure S3c). The result therefore shows that the disulphide bonds in all the moPrP variants are intact, and the differences in their stabilities are not because they differ in the oxidation status of their cysteine residues.

**pH-dependence of oligomer formation by wt moPrP.** PrP is known to form oligomers at low pH in the presence of 150 mM NaCl.[1] In the current study, the effect of pH on oligomer formation was monitored in the absence of chemical denaturants. moPrP shows a reduction in oligomer formation with increasing pH, and the pH dependence is characterized by a pKa of

~4.7 (Figure 2). This indicates that oligomer formation is linked to the protonation of a critical residue. Interestingly, several of the disease-linked mutations involve mutations of acidic amino acid residues to either neutral or basic amino acid residues.[14] The prion protein is known to traffic from outside of the cell to inside via endocytic pathway where there is a reduction in pH in lysosomes which is likely to increase the oligomerization of PrP. Not surprisingly, one plausible location for conversion of $PrP^{C}$ into $PrP^{Sc}$ that has been identified is the endocytic pathway.[15,16]

**Liposome swelling assays.** The aggregates formed at pH 2 are known to disrupt lipid membranes,[6] which points towards a putative mechanism for their toxicity. In the current study, it is shown that the oligomers formed at pH 4 also possess the same ability of disruption of lipid membranes. The oligomers formed at pH 4 indeed lead to the swelling of liposomes, an indication of pore formation in the liposomes, in a manner that is dependent on their concentration in the low micromolar concentration range (Figure S4a). 5 μM of A6 moPrP incubated for 24 h in the presence of 150 mM NaCl at 37 $^{o}$C, pH 4 showed an amplitude of liposome swelling similar to 0.1 μM of wt moPrP oligomers (data not shown) which represents (as an approximation) only a 2 % change in amplitude by A6 moPrP compared to wt moPrP.

**Fibril formation at pH 7.** Fibrilization of the moPrP variants was carried out in the presence of 2 M GdnHCl at 37 $^{o}$C, 480 rpm shaking, at 50 μM protein concentration, in the presence of 50 μM ThT in 96-well plates. Since ThT was used in the aggregation reaction, control experiments were carried out where ThT was varied from 10 μM to 500 μM keeping all other components same. The normalized aggregation plot overlapped very well and were found to be independent of ThT concentration (data not shown) which indicates that ThT does not affect the aggregation kinetics of moPrP. The final ThT fluorescence was found to be maximum for the reaction containing 50 μM ThT and hence all the further reactions were carried out at 50 μM ThT.

**References:**


1. Jain, S.; Udgaonkar, J. B. *J. Mol. Biol.* **2008**, *382*, 1228-1241.
2. Agashe, V. R.; Udgaonkar, J. B. *Biochemistry* **1995**, *34*, 3286−3299.
3. Jain, S.; Udgaonkar, J. B. *Biochemistry* **2011**, *50*, 1153-1161.
4. Singh, J.; Udgaonkar, J. B. *J. Mol. Biol.* **2013**, *425*, 3510-3521.
5. Godbole, A.; Mitra, R.; Dubey, A. K.; Reddy, P. S.; Mathew, M. K. *J. Membr. Biol.* **2011**, *244*, 67–80.
6. Singh, J.; Sabareesan, A. T.; Mathew, M.K.; Udgaonkar, J. B. *J. Mol. Biol.* **2012**, *423*, 217-231.
7. Zhang, Z.; Smith, D. L. *Protein Sci.* **1993**, *2*, 522–531.
8. Bai, Y.; Milne, J. S.; Mayne, L.; Englander, S. W. *Proteins* **1993**, *17*, 75–86.
9. Morillas, M.; Vanik, D. L.; Surewicz, W. K. *Biochemistry* **2001**, *40*, 6982-7.
10. Moulick, R.; Udgaonkar, J. B. *Biophys. J.* **2014**, *106*, 410-420.
11. Swietnicki, W.; Morillas, M.; Chen, S. G.; Gambetti, P.; Surewicz, W. K. *Biochemistry* **2000**, *39*, 424-431.
12. Maiti, N. R.; Surewicz, W. K. *J. Biol. Chem.* **2001**, *276*, 2427-2431.
13. Sang, J. C.; Lee, C. Y.; Luh, F. Y.; Huang, Y. W.; Chiang, Y. W.; Chen, R. P. Y. *Prion* **2012**, *6*, 489-97.
14. van der Kamp, M. W.; Daggett, V. *Protein Eng. Des. Sel.* **2009**, *22*, 461-468.
15. Borchelt, D. R.; Taraboulos, A.; Prusiner, S. B. *J. Biol. Chem.* **1992**, *267*, 16188-16199.
16. Arnold, J. E.; Tipler, C.; Laszlo, L.; Hope, J.; Landon, M.; Mayer, R. J. *J. Pathol.* **1995**, *176*, 403-411.

**Supplementary figures:**

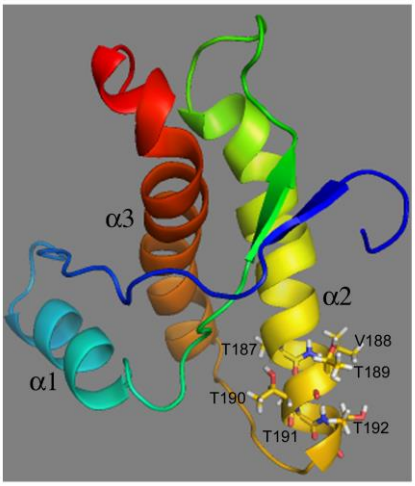


| Residue | Side-chain percent accessible surface area |
|---|---|
| T187 | 20.4 |
| V188 | 65.7 |
| T189 | 63.9 |
| T190 | 9.1 |
| T191 | 49.2 |
| T192 | 85.1 |

**Figure S1:** Structure of the C-terminal domain (residues 121 to 231) of the mouse prion protein. The residue stretch 23-121 is known to be unstructured in the full length protein. The color gradient is from blue (N-terminus) to red (C-terminus). Helix 2 (α2) stretches from residue 174 to residue 194. The residue stretch TVTTTT at the C-terminal part of α2, which was mutated in this study, is labeled. The figure was drawn using the program PyMOL and the PDB file 1AG2. The percent accessible surface areas for the side-chains of the residues in the sequence stretch TVTTTT was calculated using the NCBS integrated web server (http://caps.ncbs.res.in/iws/psa.html).

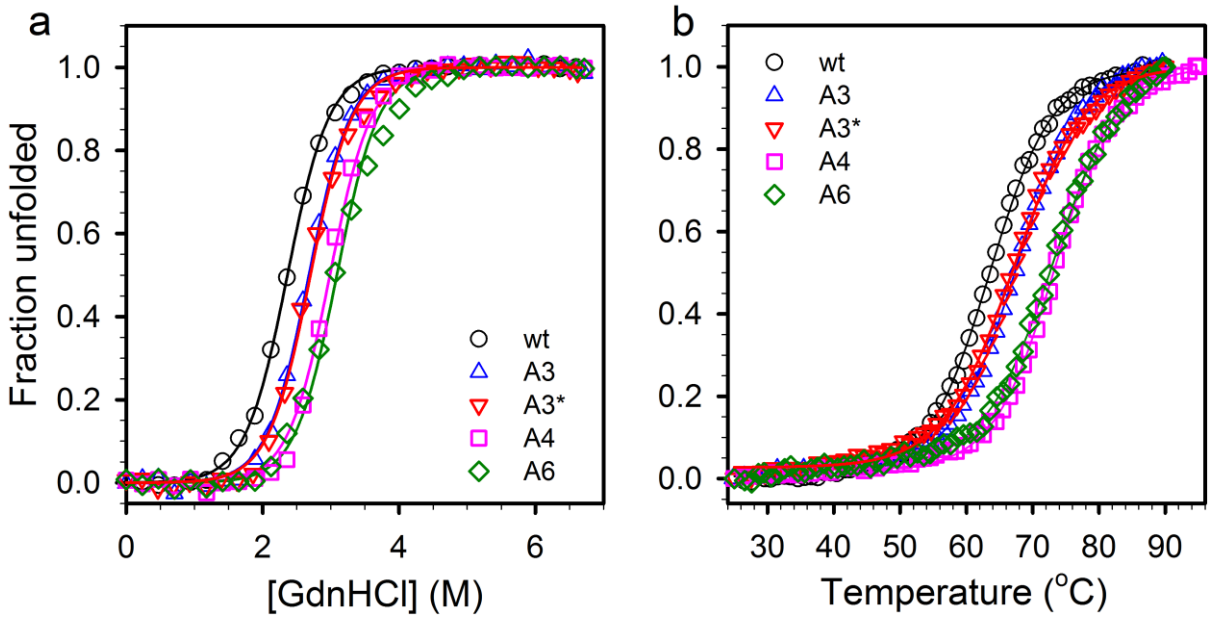


**Figure S2:** Effect of mutations on the stability of moPrP. (a) GdnHCl-induced equilibrium unfolding transitions of wt, A3, A3*, A4 and A6 moPrP at pH 7, 25 $^{o}$C as monitored by far-UV CD at 222 nm. (b) Thermal unfolding transitions of wt, A3, A3*, A4 and A6 moPrP at pH 4, as monitored by far-UV CD at 222 nm. The signal was normalized to obtain fraction unfolded.

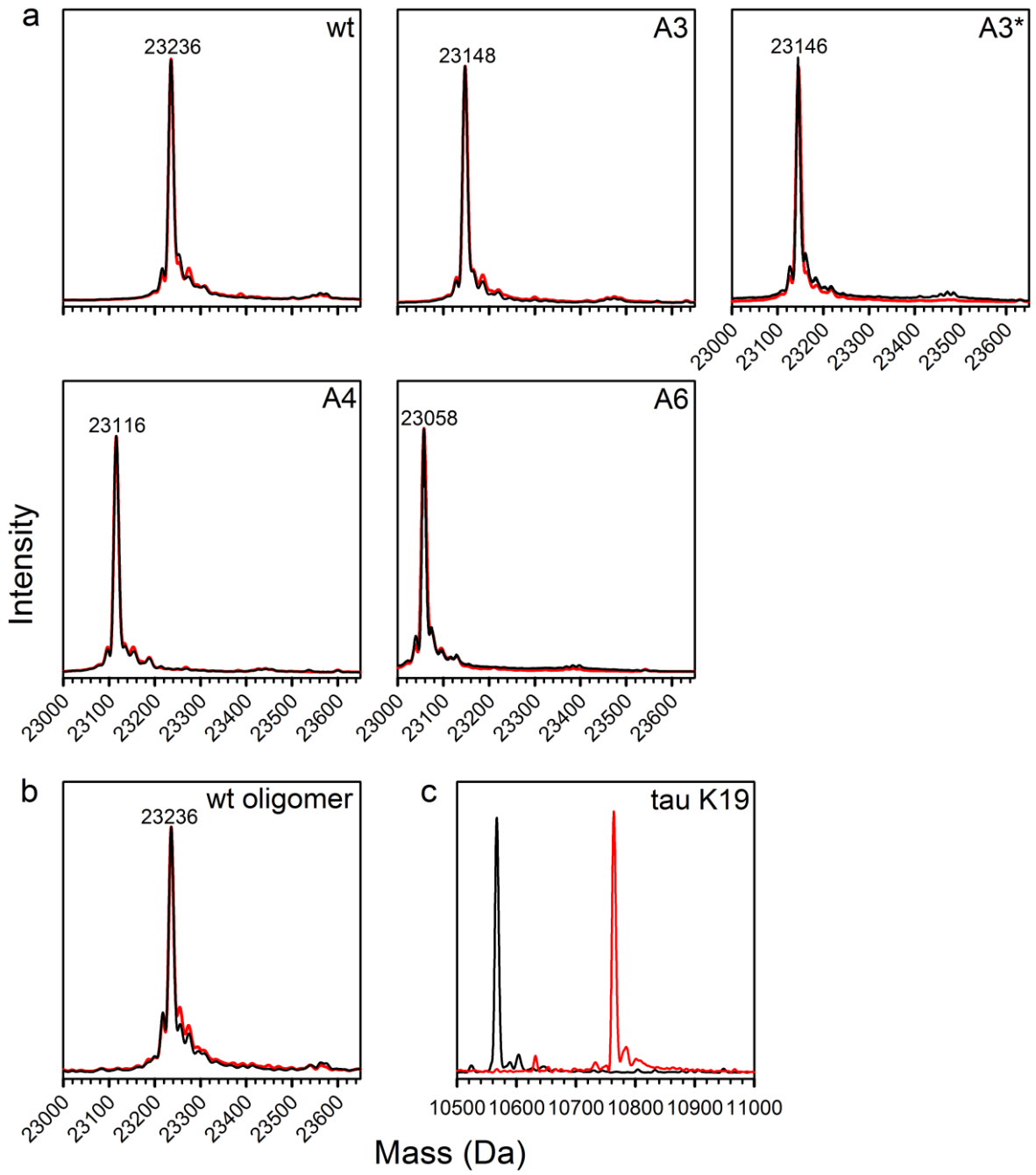


**Figure S3:** Oxidation status of the cysteine residues in the moPrP variants and oligomers. (a) Mass spectra of the moPrP variants before (black line) and after (red line) DTNB treatment in 6 M GdnHCl (see Materials and Methods). The masses of the proteins were the same as those of the untreated proteins. (b) Mass spectra of wt moPrP from oligomers after DTNB treatment. The black line shows mass spectrum of the protein where DTNB treatment of oligomers was carried out in 0 M GdnHCl while the red line shows the mass spectrum of the protein where DTNB treatment of oligomers was carried out in 6 M GdnHCl. (c) Mass-spectra of tau K19 protein before (black line) and after (red line) DTNB treatment in 6 M GdnHCl. A mass difference of +198 was observed upon labeling as expected.

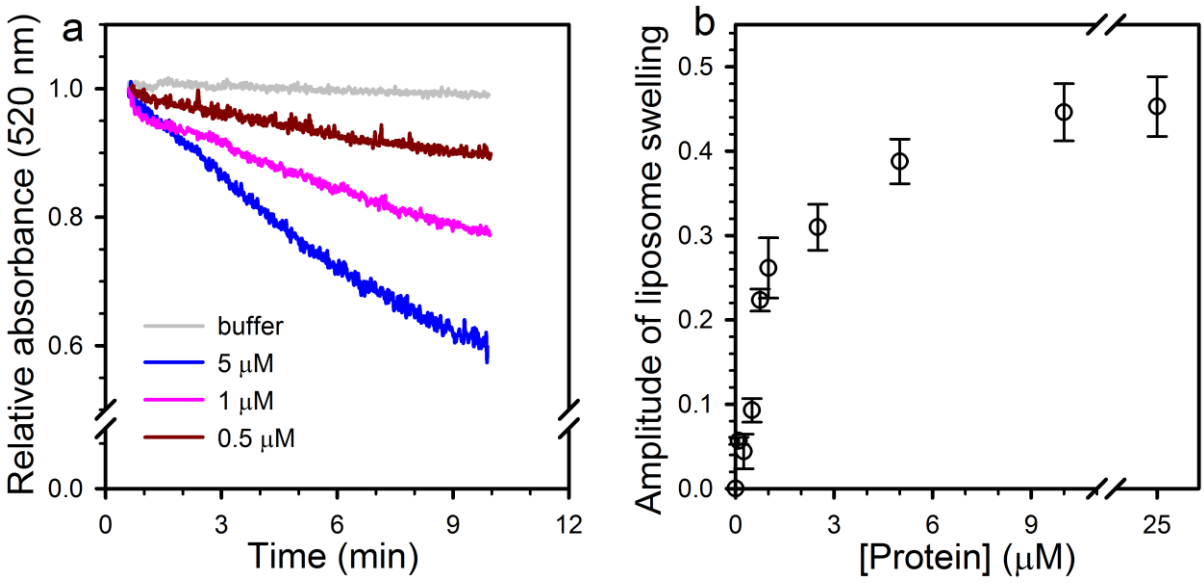


**Figure S4:** Perturbation of lipid membranes by wt moPrP oligomers at pH 4. (a) Swelling of liposomes pre-incubated with different concentrations of wt moPrP oligomers as monitored by absorbance at 520 nm upon dilution into isosmotic buffer containing PEG 1000 Da. (b) Relative amplitude of swelling of liposomes as a function of protein concentration at pH 4. The liposome swelling data (a) are shown from one batch of liposome preparation, and the extents of swelling (b) were calculated from experiments with two batches of liposomes.

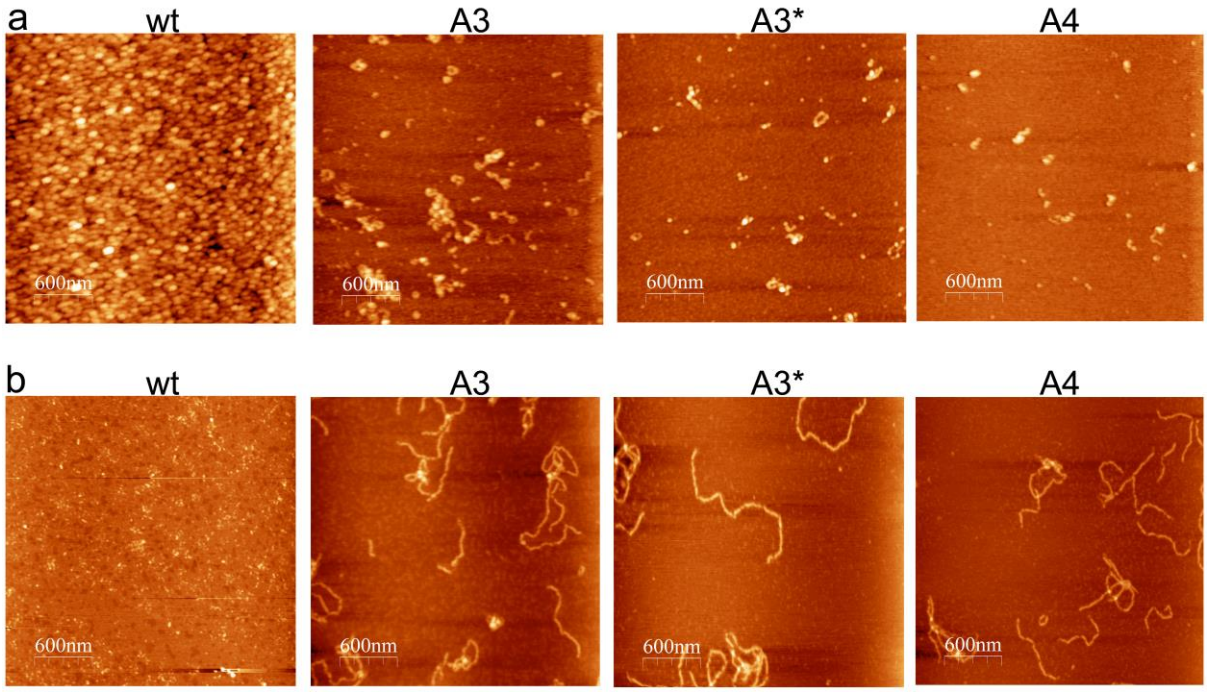


**Figure S5:** AFM images of the aggregates formed by the moPrP variants at pH 4 and pH 2. (a) AFM images of the aggregates formed by the moPrP variants at 3 days of incubation in the presence of 150 mM NaCl, at 37 $^{o}$C, pH 4 and at 100 µM protein concentration. No aggregates were observed for A6 moPrP. The Z-scale for all the images is 6 nm. The height of the oligomers (~ 2.5 nm) seen in the oligomer clumps seen for A3, A3* and A4 is the same as of the individual oligomers. (b) AFM images of the aggregates formed by the moPrP variants at 1 h of incubation in the presence of 150 mM NaCl, at 25 $^{o}$C, pH 2 and at 100 µM protein concentration. No aggregates were observed for A6 moPrP. The Z-scale for all the images is 6 nm.

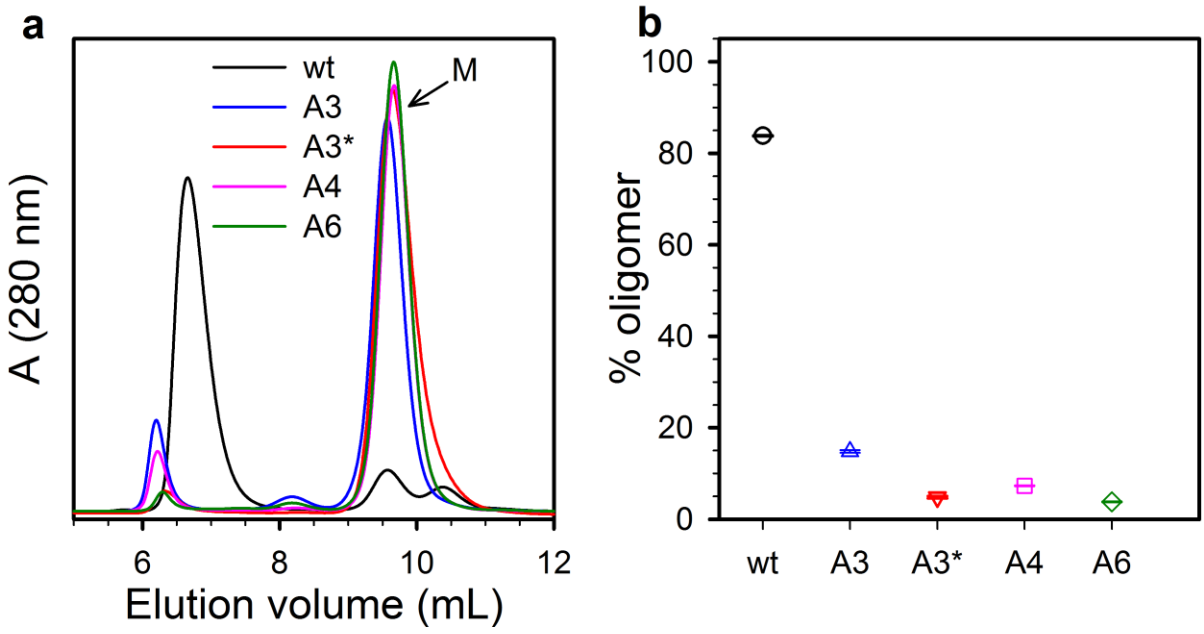


**Figure S6:** Oligomerization of moPrP variants at pH 4 in the presence of denaturants. (a) SEC profiles of different moPrP variants at 24 h of oligomerization in the presence of 150 mM NaCl, 1 M GdnHCl, 3 M urea at 37 $^{o}$C, pH 4. Label M represents the monomer peak. (b) Percent oligomer formed for moPrP variants at pH 4 in the presence of denaturants after 24 h. Error bars represent the spread in data from two independent experiments.

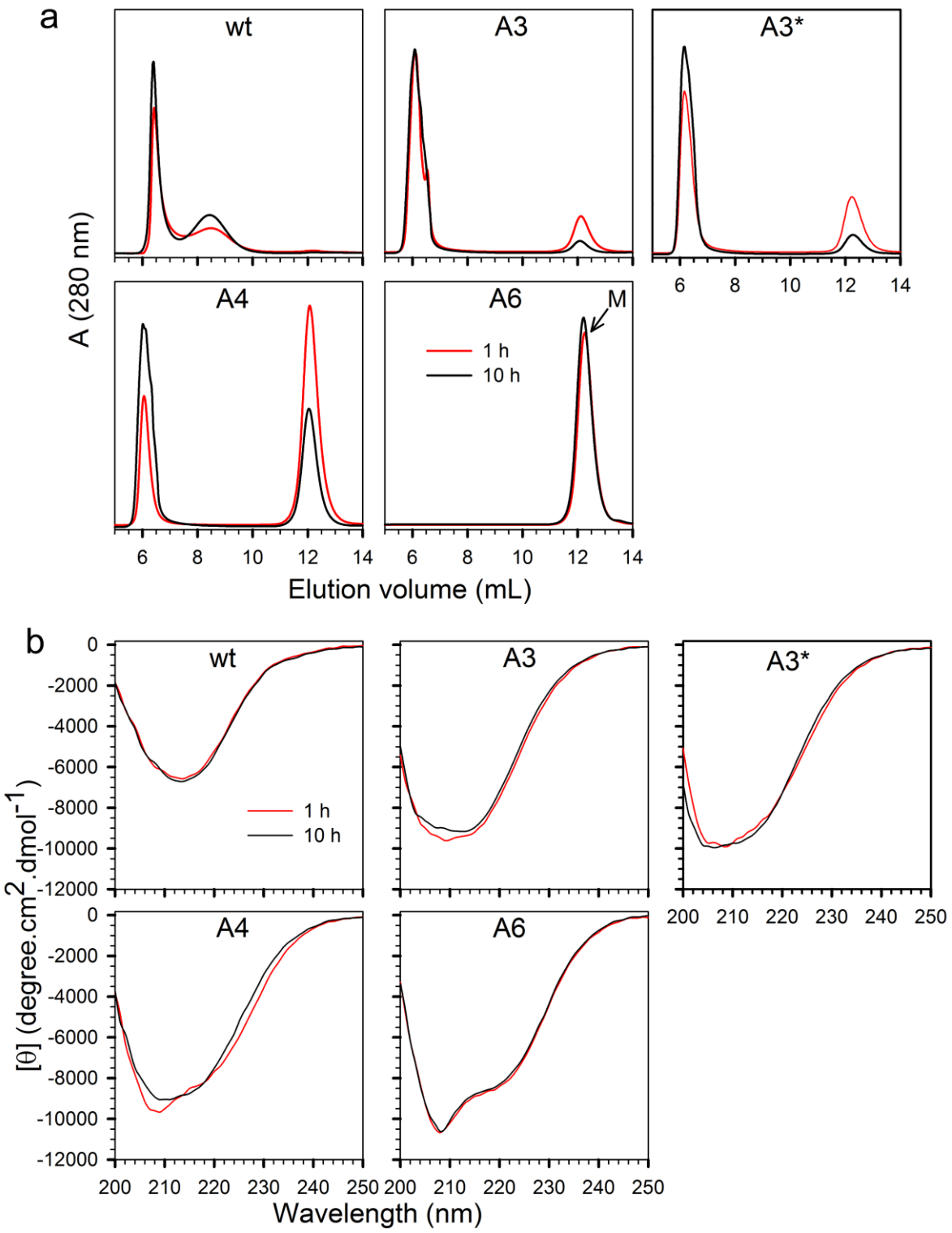


**Figure S7:** Time course of aggregate formation of moPrP variants at 100 µM concentration in 150 mM NaCl, 25 $^{o}$C, pH 2 as monitored by SEC (a) and far-UV CD (b). Label M in (a) represents the monomer peak.

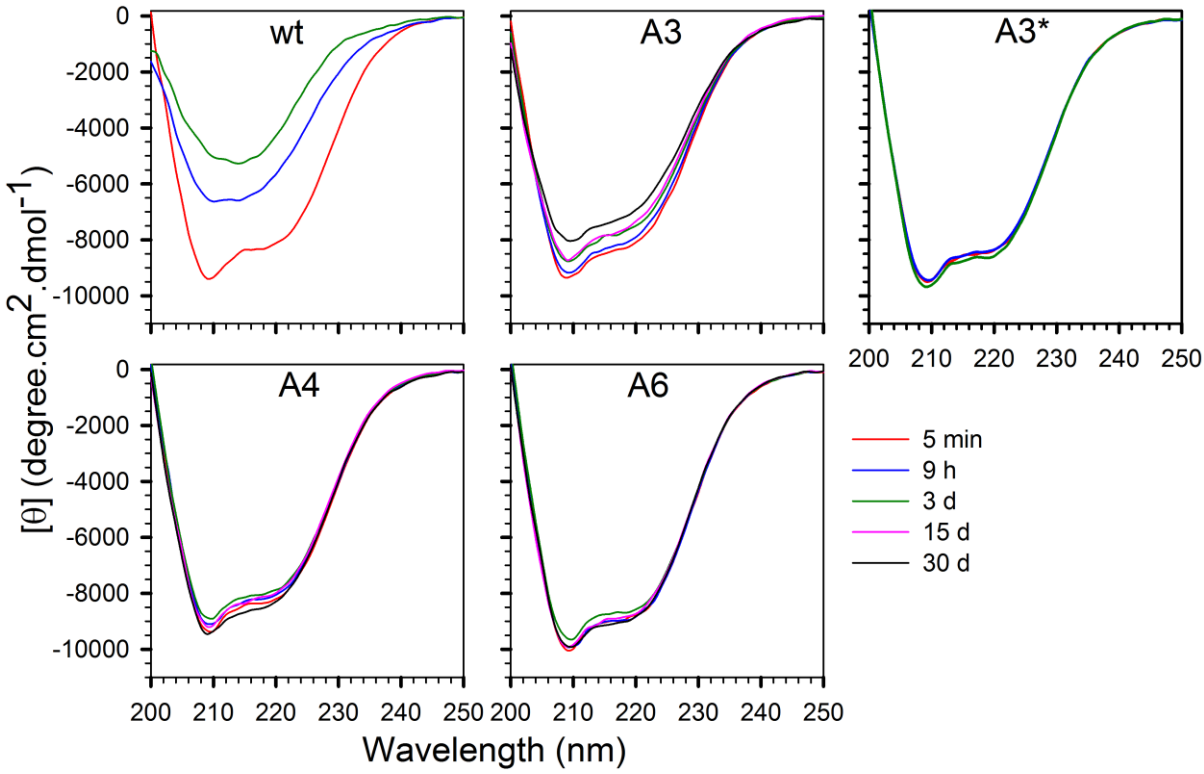


**Figure S8:** Time course of oligomerization/conformational conversion of moPrP variants in the presence of 150 mM NaCl at 37 $^{o}$C, pH 4, as probed by far-UV CD spectra.

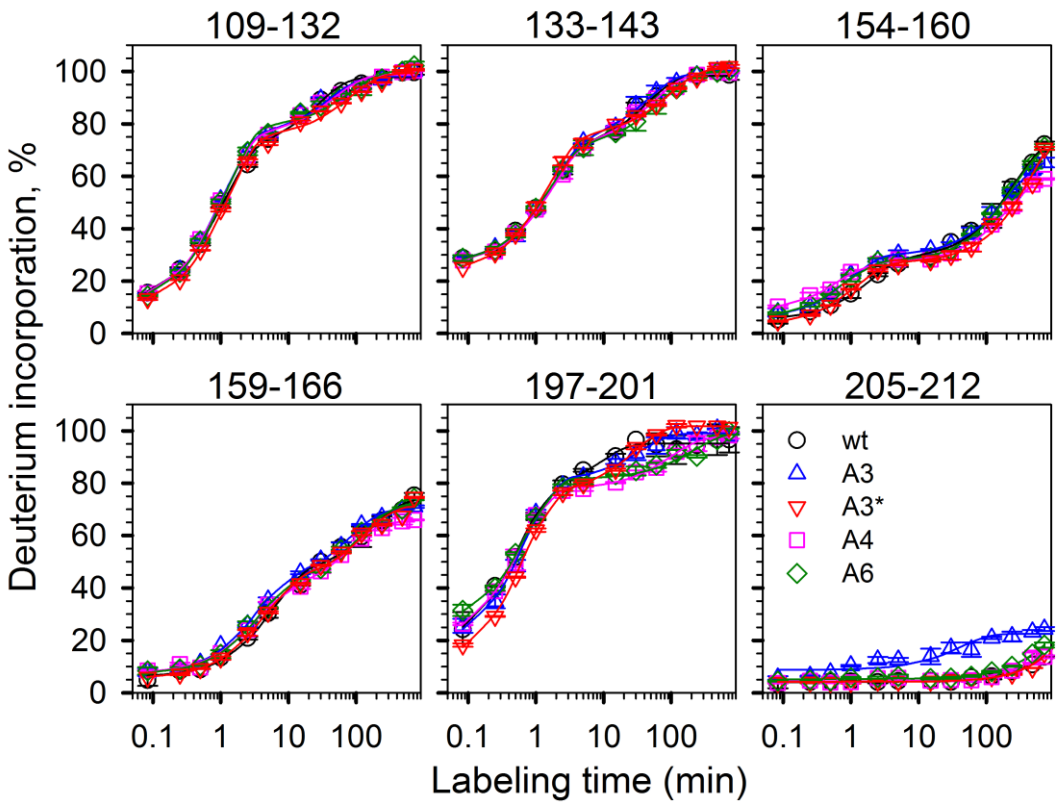


**Figure S9:** Time course of HDX in selected peptide fragments of moPrP variants at pH 4, not shown in Figure 3a. Percent deuterium incorporation profiles of different peptide fragments of wt (black circle), A3 (blue triangle), A3* (red inverted triangle), A4 (purple square) and A6 (green diamond) moPrP at 25 $^{o}$C, pH 4. Error bars represent the spread in data from two independent experiments. The lines through the data represent fits to either mono-exponential or bi-exponential curves.

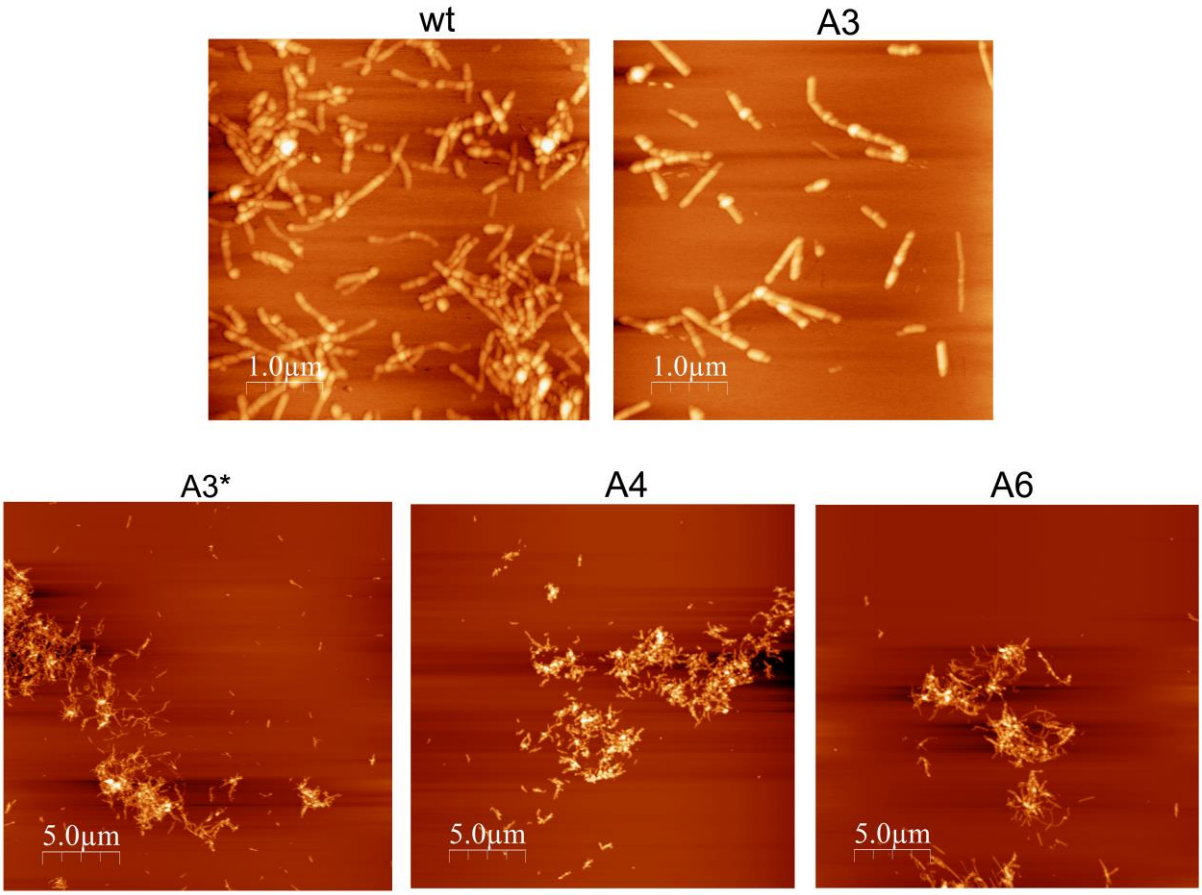


**Figure S10:** AFM images of the aggregates formed by the moPrP variants at pH 7. AFM images of the aggregates formed by the moPrP variants at 50 h of incubation in the presence of 2 M GdnHCl, at 37 $^{o}$C, 480 rpm, 50 µM ThT, pH 7 and at 50 µM protein concentration. The amyloid fibrils formed by A3*, A4 and A6 moPrP formed clumps and hence, a larger scale was used for imaging the amyloid fibrils formed by these variant proteins.

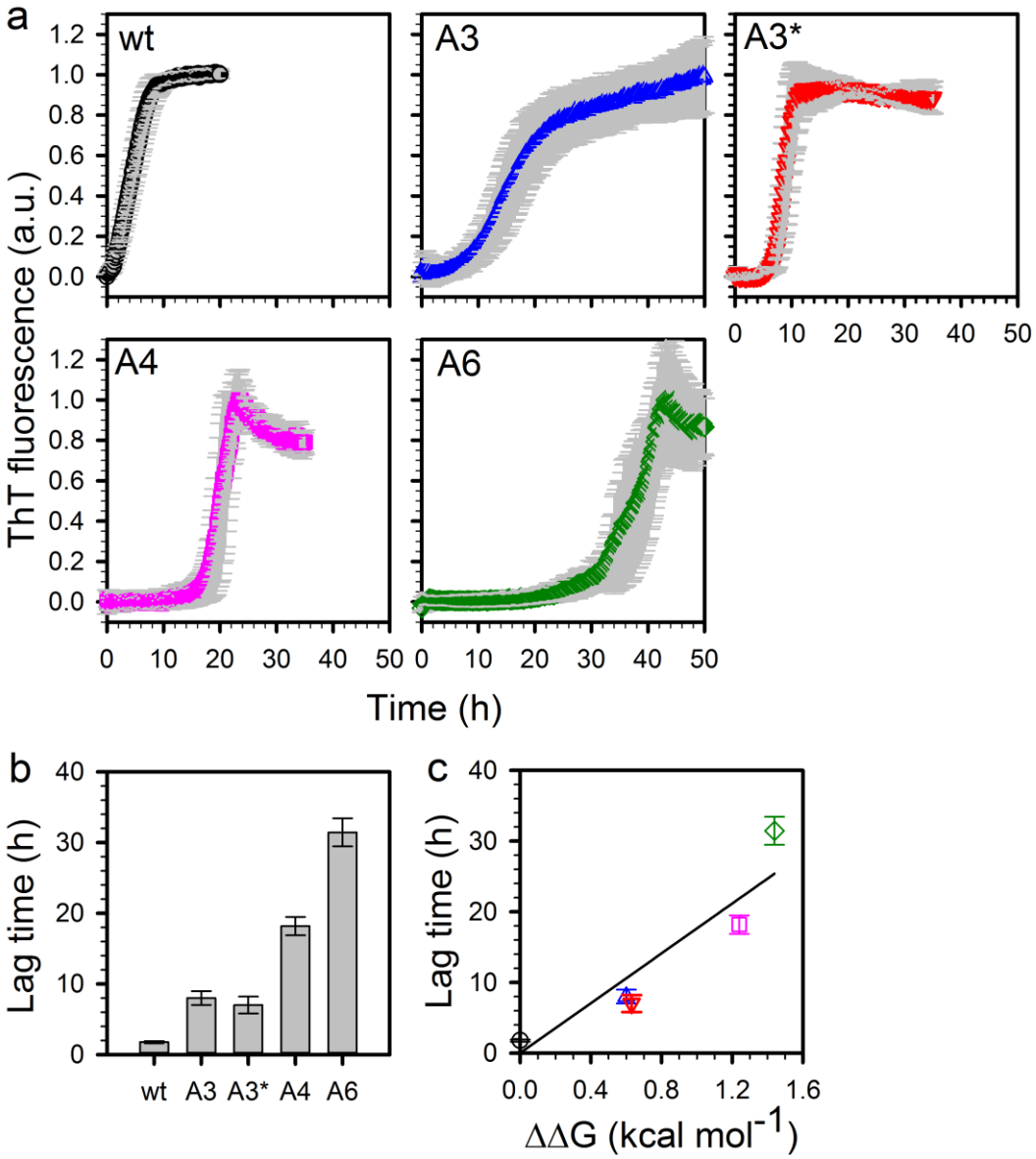


**Figure S11:** Effect of mutations on fibril formation of moPrP at pH 7. (a) Kinetics of fibril formation by the moPrP variants probed by ThT fluorescence measurements. (b) Lag time of fibril formation for the different moPrP variants. (c) Lag time of fibril formation for the different moPrP variants is plotted against the increase in stability (ΔΔG) over that of wt moPrP at pH 7. The symbol and colors in (c) are the same as in (a). See Table S2 for the ΔΔG values for the different moPrP variants. Error bars (grey) represent the spread in data from three independent experiments with 5 wells for each reaction in each experiment.

**Table S1:** Thermodynamic parameters obtained from urea-induced equilibrium unfolding and thermal unfolding studies of different moPrP variants at pH 4.

| Protein | ΔG (kcal $mol^{-1}$) | ΔΔG (mutant-wt) | $C_m$ (M) | $\Delta C_m$ (M) (mutant-wt) | $T_m$ ($^oC$) | $\Delta T_m$ (mutant-wt) |
|---|---|---|---|---|---|---|
| **wt** | 4.12±0.10 | | 3.35±0.09 | | 63.5 | |
| **A3** | 4.48±0.14 | +0.36 | 3.63±0.11 | +0.28 | 67.6 | +4.1 |
| **A3*** | 4.85±0.04 | +0.73 | 3.94±0.03 | +0.59 | 67.2 | +3.7 |
| **A4** | 5.09±0.12 | +0.97 | 4.14±0.10 | +0.79 | 73.3 | +9.8 |
| **A6** | 5.43±0.11 | +1.31 | 4.41±0.09 | +1.06 | 73.2 | +9.7 |

The m value was constrained to 1.23 kcal $mol^{-1}$ $M^{-1}$ for all the moPrP variants.

**Table S2:** Thermodynamic parameters obtained from GdnHCl-induced equilibrium unfolding studies of different moPrP variants at pH 7.

| Protein | ΔG (kcal $mol^{-1}$) | ΔΔG (mutant-WT) | Cm (M) | ΔCm (mutant-WT) |
|---|---|---|---|---|
| **wt** | 4.56±0.05 | | 2.36±0.02 | |
| **A3** | 5.16±0.01 | +0.60 | 2.68±0.01 | +0.32 |
| **A3*** | 5.19±0.02 | +0.63 | 2.69±0.01 | +0.33 |
| **A4** | 5.80±0.04 | +1.24 | 3.01±0.02 | +0.65 |
| **A6** | 6.00±0.04 | +1.44 | 3.11±0.02 | +0.75 |

The m value was constrained to 1.93 kcal $mol^{-1}$ $M^{-1}$ for all the moPrP variants.